Polymer Nanostructures Made by Scanning Probe Lithography: Recent Progress in Material Applications

Zhuang Xie, Xuechang Zhou, Xiaoming Tao, Zijian Zheng*

Scanning probe lithography (SPL) is a series of techniques that utilizes a scanning probe or an array of probes for surface patterning. Recent developments of new material systems and patterning approaches have made SPL a promising, low-cost, bench-top, and versatile tool for fabricating various polymer nanostructures, with extraordinary importance in physical sciences, life sciences and nanotechnology. This feature article highlights the recent progress in four material applications: polymer resists, polymeric carriers for patterning functional materials, electronically active polymers and polymer brushes for tailoring surface morphology and functionality. An overview of future possibilities, with regard to challenges and opportunities in this field, is given at the end of the paper.

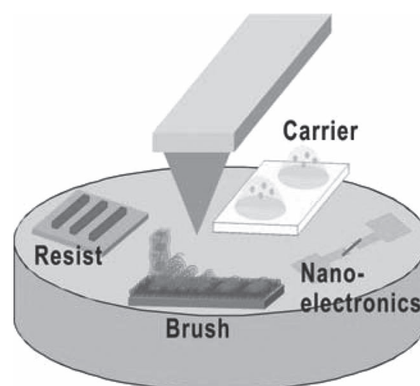

1. Introduction

Polymer materials with a length scale of 1–100 nm have shown many properties superior to its bulk. As such, the manipulation of polymers at their nanosized interfaces has become an ever-increasingly important issue in physical sciences, life sciences and nanotechnology.[1] Among the existing lithographic technologies for creating nanoscale structures, scanning probe lithography (SPL) is a powerful, versatile and easily accessible tool to realize both precise spatial fabrication and in situ imaging of structures at the nanometer, and even at the molecular level. Utilizing sharp scanning tips attached to a piece of equipment, such as a scanning tunneling microscope (STM), an atomic force microscope (AFM), a scanning electrochemical microscope (SECM), or a scanning near-field optical microscope (SNOM),[2] SPL offers maskless and template-free manufacturing of arbitrary nanostructures with ultrahigh resolution and registration. Moreover, with the advantages of being relatively low-cost, capable of operation in ambient conditions and having good compatibility with soft matter, SPL is often used in the fabrication of polymer nanostructures for a wide range of applications.

In the past two decades, scanning probes delivering either energy or materials have provided a wide variety of approaches for making polymer nanostructures.[3] Early versions of SPL for soft materials were "destructive", the surface materials being removed or modified by applying external mechanical, thermal, electrical or optical energy through the scanning probe. Typical examples include nanoploughing,[4] nanoshaving,[5] thermomechanical indentation,[6] thermochemical nanolithography,[7] electrostatic nanolithography,[8] electrochemical oxidation[9] and SNOM-based photolithography.[10] The invention of dip-pen nanolithography (DPN)[11] in 1999 by Mirkin's group opened up possibilities for "constructive" SPL, which delivers materials with an inked scanning probe directly, forming surface architectures.[3a,12] A number of variants of DPN have been developed to extend the capabilities

Z. Xie, Dr. X. Zhou, Prof. X. M. Tao, Prof. Z. J. Zheng
1. Nanotechnology Center, Institute of Textiles and Clothing, The Hong Kong Polytechnic University, Hong Kong SAR, China;
E-mail: tczzheng@inet.polyu.edu.hk
Z. Xie, Dr. X. Zhou, Prof. X. M. Tao, Prof. Z. J. Zheng
Advanced Research Centre for Fashion and Textiles, The Hong Kong Polytechnic University, Shenzhen Research Institute, Shenzhen, China

© 2012 WILEY-VCH Verlag GmbH & Co. KGaA, Weinheim

DOI: 10.1002/marc.201100761

of constructive SPL further by combining the DPN with additional stimuli such as forces,[13] heat[14] and electric fields,[15] as well as integrating AFM tips with microfluidic systems.[16]

The literature on the subject of creating polymer nanostructures by SPL before 2008 was thoroughly reviewed by Lee and Sheehan.[17] In the last 3 years (2008–2011), enormous progress has been made in SPL techniques, addressing more practical and complex challenges that are broadly categorized in the following: 1) scanning probes have become competent in the delicate manipulation of functional materials for the generation of complicated surface nanoarchitectures, the precise control of polymer functionality with well-defined composition, morphology or interactions, and, more importantly, the use of those tailored structures and functions in fundamental studies, as well as device applications; 2) with the advances in the parallelization of scanning probe arrays, including cantilever-based[18] and more recent cantilever-free[19] configurations, the capabilities of SPL have been expanded to enable high-throughput production of polymer nanostructures over large areas.

In view of the rapid growth in this field (Figure 1), this Feature Article aims at highlighting the latest developments (since 2008) in the fabrication of polymer nanostructures via SPL on the route to different applications, although some previous attempts before 2008 on this topic will be mentioned without deep elaboration. We categorize the recent progress into four material applications, including polymer resists for nanofabrication, polymeric carriers for functional materials, electronically active polymers and polymer brushes. A summary of the developments in SPL and an indication of the future challenges and opportunities in this field are subsequently provided.

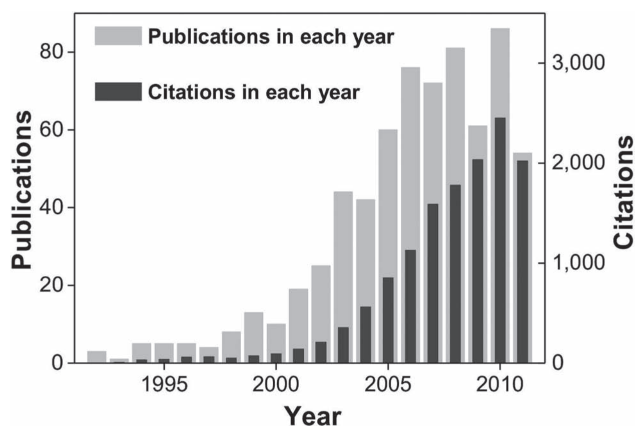

Figure 1. Numbers of papers published each year since 1991 concerning SPL for the fabrication of polymer nanostructures, and the numbers of citations in each year. The data was adopted from the ISI Web of Science database.

Zhuang Xie received his B.S. in chemistry at Renmin University of China in 2010. Currently, he is a postgraduate student pursuing his PhD degree at the Nanotechnology Center of the Institute of Textiles and Clothing, The Hong Kong Polytechnic University. His work in Prof. Zijian Zheng's group includes scanning probe lithography, engineering of surface polymer structures and wearable electronic devices.

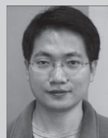

Dr. Xuechang Zhou received his B.S. in polymer chemistry at the University of Science and Technology of China in 2005, and MPhil and PhD degrees in chemistry at the Chinese University of Hong Kong in 2007 and 2010, respectively. His graduate work involved the use of microfluidic systems for the study of protein crystallization, enzymatic assay and polymer phase diagrams. He is currently a Postdoctoral Fellow in Prof. Zijian Zheng's group at The Hong Kong Polytechnic University, working on the construction of surface architectures with polymer brushes at the micro- and nanoscale. His research interests include microfluidics, analytical chemistry, polymer science and scanning probe nanolithography.

Prof. Xiaoming Tao is Chair Professor of Textile Technology, Institute of Textiles and Clothing, The Hong Kong Polytechnic University. She obtained a BEng in textile engineering from the East China Institute of Textile Science and Technology and a PhD in textile physics from the University of New South Wales in Australia. Her research work is focused on intelligent fibrous materials, nanotechnology, photonic fibres and fabrics, flexible electronic and photonic devices, yarn manufacturing and textile composites.

Prof. Zijian Zheng is currently an Assistant Professor of the Institute of Textiles and Clothing at The Hong Kong Polytechnic University. His research interests include the development of surface patterning techniques, synthesis and application of graphene-based materials, structuring polymer architectures, and wearable electronic devices. Prof. Zheng received his BEng in Polymer Materials and Engineering from the Department of Chemical Engineering at Tsinghua University (Beijing) in 2003. He joined Prof. Wilhelm T. S. Huck's group in 2004 and received his PhD degree in Chemistry at the University of Cambridge (UK) in 2007. His PhD thesis involved the development and application of surface patterning techniques for tailoring surface functionality. From January 2008 to June 2009, he worked in Prof. Chad A. Mirkin's group as a Postdoctoral Research Fellow at Northwestern University (US) focusing on the development of scanning probe nanolithography (e.g., polymer-pen lithography (PPL)).

© 2012 WILEY-VCH Verlag GmbH & Co. KGaA, Weinheim

2. Polymer Resists for Nanofabrication

Polymer resists play an irreplaceable role as templates in nanofabrication. Unlike conventional photolithography and electron-beam lithography (EBL), SPL allows the maskless formation of patterned polymer resists at ambient conditions. SPL also has the potential of becoming a low-cost nanofabrication tool. In recent years, patterning polymer resists by SPL has gained considerable advances as a result of the development of new, parallel SPL techniques and new resist materials.

Photoresists are the most commonly used polymer resist in nanofabrication. Scanning near-field optical lithography (SNOL), a probe-based optical lithography method that is achieved by coupling a UV light source to SNOM, has been developed for site-selective photochemical degradation or transformation of photosensitive materials.[10] Using SNOL, a resolution of 35 nm on a positive photoresist is now possible, which is less than 1/10 of the wavelength of the incident light.[20] Recently, Leggett and coworkers reported the development of parallel SNOL using a 1D array of SNOM probes, and the technique was named "Snomipede" by the research group (Figure 2A–C).[21] In Snomipede, a series of light beams are focused and pass through optical windows on the probe, where each beam can be switched ON or OFF independently. The probe

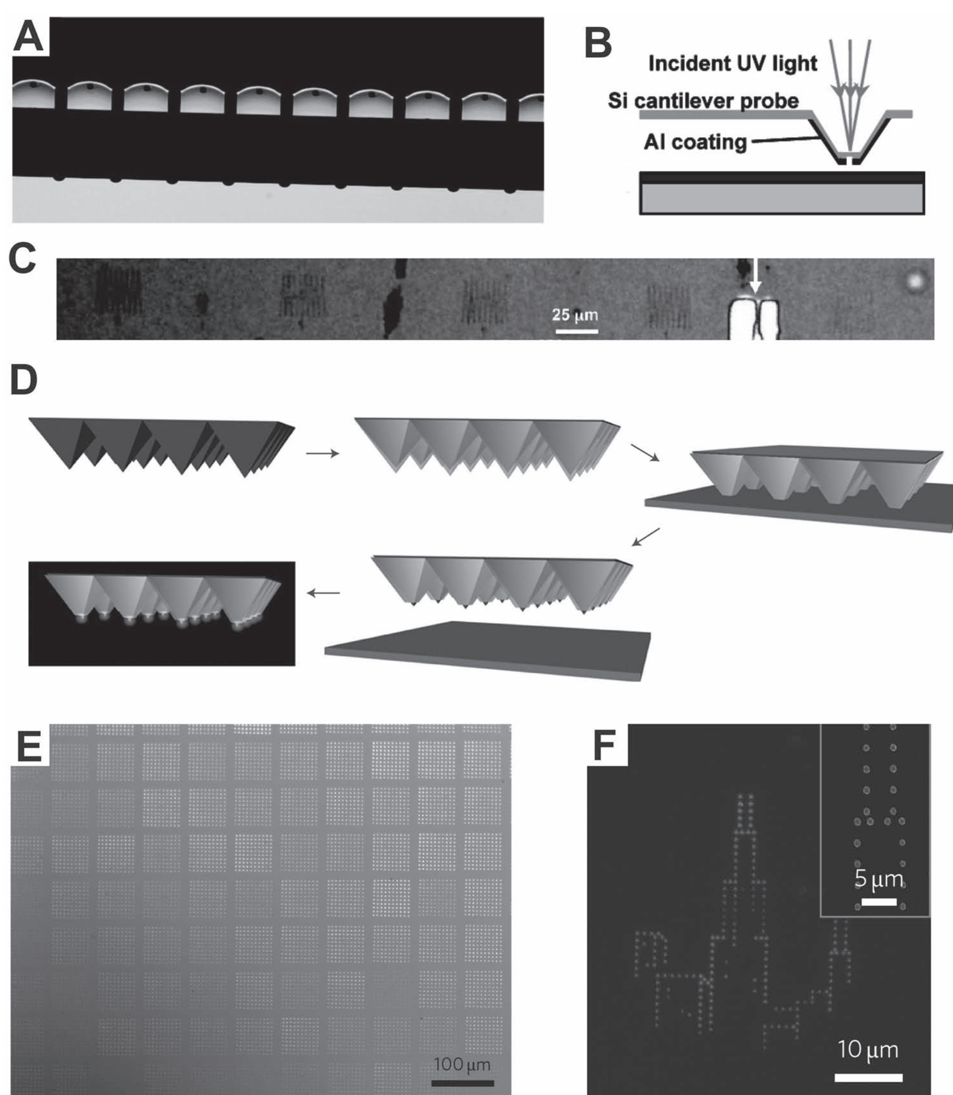

Figure 2. Parallel SNOL on a photoresist. A) Optical image of a Snomipede array. B) The configuration of one SNOM probe in a Snomipede array. C) Optical image of a parallel array of line patterns on a photoresist fabricated using Snomipede. Reproduced with permission.[21] Copyright 2010, American Chemical Society. D) Schematic illustration of the fabrication process of a cantilever-free tip array for BPL. The PDMS tip array coated with Au is brought into contact with an adhesive poly(methyl methacrylate) (PMMA) surface to remove the Au layer from the apex of each tip and create an aperture. E) Large-area Au dot arrays made by BPL (after metal evaporation and photoresist lift-off). F) An arbitrary Au pattern fabricated by BPL. Reproduced with permission.[22] Copyright 2010, Nature Publishing Group.

© 2012 WILEY-VCH Verlag GmbH & Co. KGaA, Weinheim

array has the advantage that individual probes within the array can be operated independently as writing or non-writing pens, leading to the generation of different patterns from different probes in a parallel writing process. The Snomipede technique was also demonstrated to work underwater, producing photoresist nanofeatures down to 70 nm. On the other hand, a cantilever-free SPL technique, namely beam pen lithography (BPL), has been developed for patterning photoresists in a similar fashion (Figure 2D–F).[22] BPL uses a cantilever-free 2D array of pyramidal tips made of polydimethylsiloxane (PDMS). Instead of using microfabrication techniques to punch a hole all the way through a silicon-based cantilever, as is the case of SNOL, BPL forms the pathway for light illumination by simply coating a transparent polymer-tip array with an opaque metal layer and subsequently removing the metal layer at the tip end. Precise control of the distance between the pen array and the substrate by AFM allows either near- or far-field optical lithography to produce sub-diffraction-limit or micrometer-sized patterns in arbitrary forms, with the smallest size approaching 100 nm. When compared with the Snomipede technique, it may be seen that the tip array of BPL is largely scalable and the cost is low, although active-type BPL is yet to be demonstrated.

A second type of polymer resist suitable for SPL is that of a thermally sensitive polymer that undergoes conformational rearrangement or chain degradation after tip-induced, localized heating. The Millipede project, which utilizes a 2D active AFM cantilever array, is the most well known, early example of a technique used to achieve this.[18a] In recent research, thermomechanical indentation using Millipede tips and specially designed crosslinked polymer resists have achieved sub-10-nm features, which can be used for high density data storage.[23] Knoll and coworkers further developed a novel self amplified depolymerization (SAD) polymer resist as an easily removable template for thermochemical nanolithography, in which the SAD polymer decomposes into monomers without leaving debris when heated.[24] More importantly, the SAD polymer resist has served as an ideal method for top-down manufacturing of 3D nanostructures by means of SPL (Figure 3).[25] Since the heat-induced decomposition of SAD polymers is accomplished within a few microseconds, the reaction timescale is faster than the mechanical motion of the tip and the force required to penetrate the film can be ignored. As a consequence, the depth of the removed region has been found to have a linear relationship with applied load, and 3D nanolithography on an SAD polymer resist by SPL can be achieved in a single patterning step, rather than by multicycle, layer-by-layer removal of materials.[26] As proof-of-concept, a 3D topographic world map with 5×10^5 pixels was engraved at a pitch of 20 nm by linearly transforming the elevation data into force information. The whole process took just 143 s, showing the high efficiency of probe-based 3D nanofabrication.

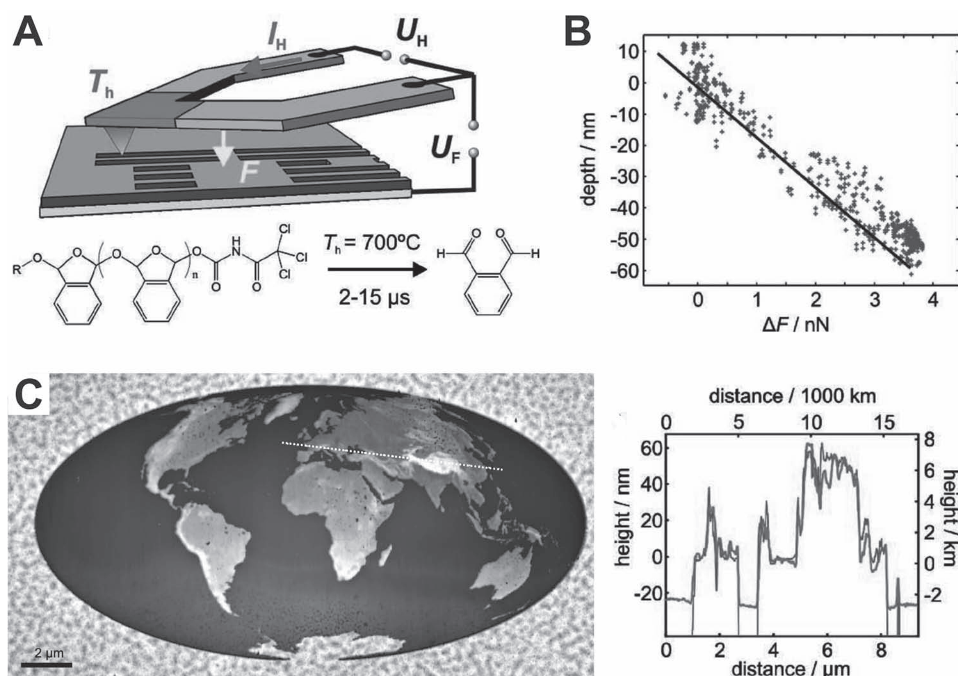

Figure 3. A–C) Probe-based 3D thermochemical nanolithography: schematic illustration of the thermochemical nanolithography based on SAD polymers (A); plot of the patterning depth as a function of applied force (B); AFM topography of a 3D world map written by transposing the height information of the original data into a force, the right-hand-side image showing cross-section profiles along the dotted line (C). Reproduced with permission.[25]

© 2012 WILEY-VCH Verlag GmbH & Co. KGaA, Weinheim

The third type is that of a polymer that can be additively transferred from the tip to the substrate. DPN patterning of poly(ethylene glycol) (PEG) is the most representative example.[27] PEG absorbs a large amount of water at a high humidity and becomes a viscous liquid. It is considered to be liquid ink (compared with traditional molecular ink) for DPN patterning, during which the "liquid" PEG flows onto the substrate at the tip-substrate contact areas. Being "liquid", the shape of the PEG feature is spherical-cap-like, similar to that of a water drop on a substrate, and the thickness and contact angle of the PEG spherical caps are related to the surface energy of the substrate. Since the first report on the topic in 2008, SPL patterning of PEG has been achieved using single cantilever DPN, 1D cantilever array DPN, and cantilever-free, 2D polymer pen lithography (PPL) for various applications (Figure 4). For example, combining with the metal-evaporation, etching and lift-off process, PEG micro-/nanostructures made by

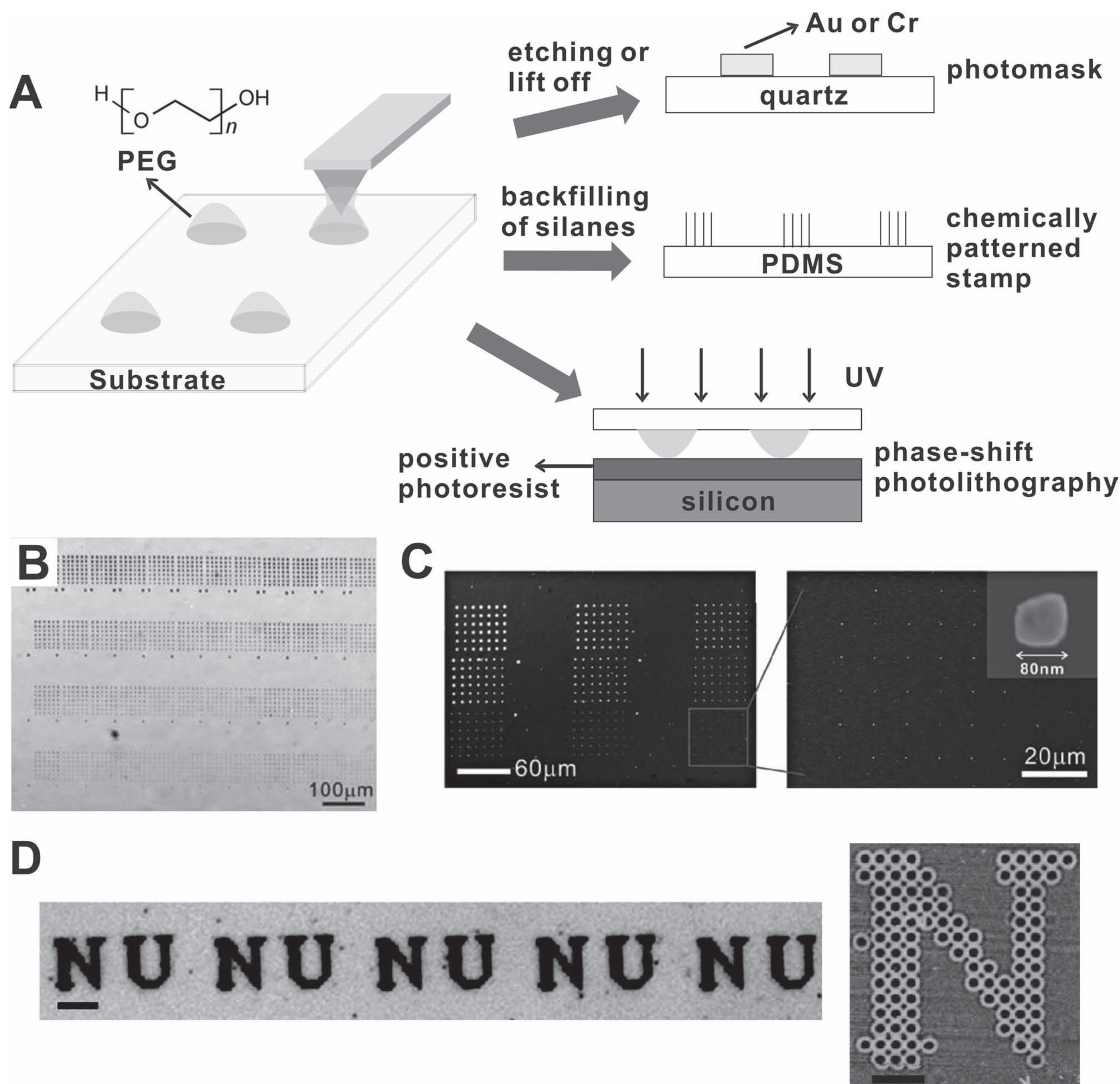

Figure 4. PEG resist fabricated by DPN for multifunctional applications. A) Schematic illustration of the fabrication and application of a PEG resist. B) Optical image of DPN-generated PEG arrays on PDMS. C) Sub-100-nm Au dot arrays from microcontact printing with chemically patterned, flat PDMS stamps. Reproduced with permission.[29] D) Optical image of an array of arbitrary photoresist patterns fabricated with PEG phase-shift lenses. The AFM image to the right shows that the letter "N" consists of well-shaped features. The scale bars are 20 μm and 5 μm, respectively. Reproduced with permission.[30] Copyright 2010, American Chemical Society.

© 2012 WILEY-VCH Verlag GmbH & Co. KGaA, Weinheim

means of DPN have been used as a form of sacrificing resist for fabricating photomasks on quartz.[28] In another example, Zheng et al. fabricated PEG nanostructures with DPN on flat PDMS as a resist for plasma treatment.[29] After backfilling of various silane molecules on the unprotected areas and removal of the PEG resist, a topographically flat PDMS stamp with well-defined chemical regions was formed, which could be used for microcontact printing of small molecules, proteins and polar inks at sub-100 nm. Furthermore, since DPN-deposited PEG dots on glass are hemispheric and transparent, they possess optical properties and can be employed as nanosized lenses for subwavelength photolithography:[30] parallel light passing through PEG was focused beneath the center of the PEG lens, with a lower intensity at the edges. Jang et al.[30] demonstrated that arrays of PEG lenses on glass function as phase-shift photomasks for making well- or ring-shaped structures on positive photoresists. Other types of liquid polymer inks such as PDMS have also been transported by DPN and used as polymer resists or masters after the curing process.[31]

3. Polymeric Carriers for Functional Materials

One challenge of SPL is how to fabricate functional nanostructures, such as biomolecules and inorganic crystals. Previous attempts have focused on a two-step process by firstly creating templates via SPL and subsequently immobilizing these functional materials. Recently, with the development of direct deposition of polymer materials by the DPN and PPL techniques, which are elaborated upon in the above, a one-step strategy using a polymer carrier has been developed. The innovation is that functional materials (such as proteins) or precursors of functional materials (such as inorganic salts for metallization), which are difficult to transfer directly by an AFM tip, were mixed with a mobile polymer. The mixture was then used as an ink for patterning by DPN and PPL, in which the polymer acted as cargo matrix to carry the functional material onto the substrate.

A hydrogel carrier matrix was first reported by Mirkin's group using agarose to facilitate the delivery of large biomolecules, such as proteins and oligonucleotides (Figure 5A–C).[32] The deposition rate was found to be as high as three orders of magnitude faster than normal DPN writing with pure biomolecular ink. After covalent bonding with the surface, the bioactive structures were retained on the substrate after washing away the agarose with water. PEG has also been universally utilized as a carrier in the matrix-assisted deposition of functional materials (Figure 5D–F).[33,34] Both DPN and PPL experiments have been demonstrated to pattern nanostructures of PEG matrixes loaded with nanoparticles (NPs), C_{60} or biomolecules onto different substrates. Importantly, the nanomaterials were active after removing the PEG by means of water rinsing or O_2 plasma. For example, C_{60} still worked as a conductive material in a photoresponsive device after the polymer matrix had been removed using O_2 plasma. Enzyme nanostructures transferred by PEG could effectively degrade poly(L-lactic acid) films site-specifically.[34] Another key advantage of the polymer carrier system is that it can modulate the transport rate of the polymer/functional material mixture because the transport characteristics of the polymer carrier dominate the system. This is especially important for achieving a similar feature size using different inks in the multiplex patterning of biological materials. For example, by using an agarose carrier, an identical spot size was achieved for two different proteins (cholera toxin β (CTβ) and immunoglobulin G (IgG)), which were patterned under the same conditions (Figure 5B). Combined with a massively parallel tip array, it is promising for printing multiplexed biomolecular nanostructures with extremely high speeds and densities.[35]

As well as hydrogels and PEG, Chai et al. adopted block copolymers as both the delivery matrix and a nanoreactor for site-selective synthesis of nanoparticles (Figure 5G–H).[36] Poly(ethylene oxide)-*block*-poly(2-vinylpyridine) (PEO-*block*-P2VP) was chosen as the preferred material because the PEO block promotes ink transport while the P2VP block has a high association interaction with $AuCl_4^{-1}$ ions, which show weak solubility in PEO. Unlike the blending situation in the hydrogel matrix, the block copolymer formed micelles in the solution, where a small quantity of metal ions was localized inside the P2VP core. After patterning the micelles on substrates by DPN and PPL, the polymer matrix was removed by means of O_2 plasma, leaving arrays of single-crystalline metal nanoparticles as small as 4.8 nm.

The use of polymer matrices has been extended to other water-insoluble polymers. Sheehan and coworkers exploited a number of thermoplastic polymer matrices to transport nanoparticles using thermal DPN.[37] The nanocomposites deposited from a heated probe included PMMA/Fe_3O_4, polyethylene/quantum dots, polyvinylidene fluoride trifluoroethylene (PVDF-TrFE)/tris(8-hydroxyquinolinato)aluminium (Alq_3), conjugated polymer/Au and other combinations. The molten polymers formed uniform and dense features encapsulating well-dispersed nanoparticles. After plasma removal of the polymers, the final nanoparticle lines could approach single particle resolution. A photocurable host matrix has also been developed to transfer photoluminescent truxenes.[38] Instead of removing the matrix, the deposited carrier liquid was UV cured to serve as a capping matrix, in which the truxenes were protected from losing their activity.

4. Electronically Active Polymers

Nanopatterning of electronically active polymers, including conducting polymers, semiconducting polymers and

© 2012 WILEY-VCH Verlag GmbH & Co. KGaA, Weinheim

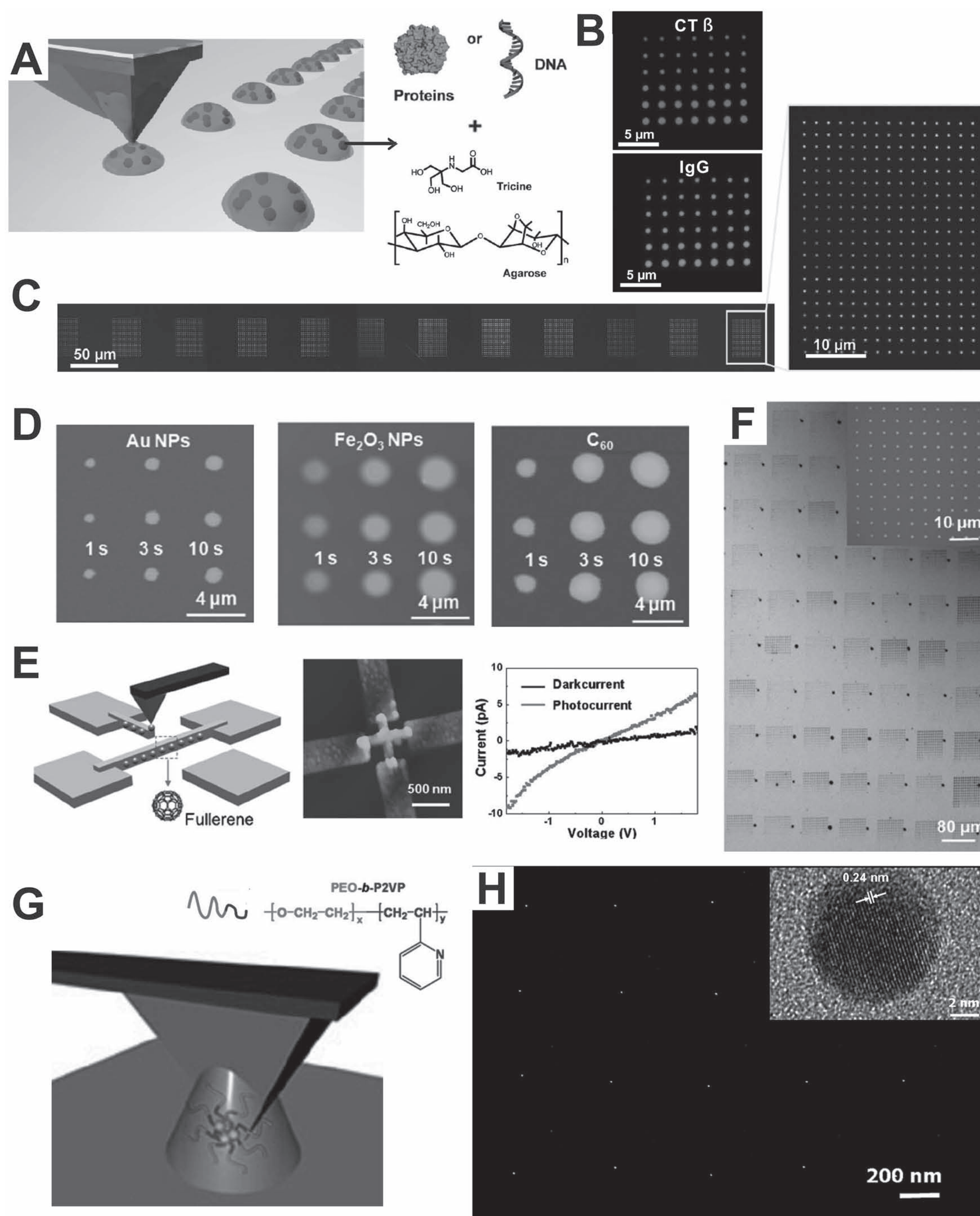

Figure 5. Polymer carrier matrixes. A) Schematic illustration of DPN patterning of agarose/biomolecules mixtures. B) Fluorescent images of two patterned proteins, CTß and IgG, showing similar feature sizes. C) Parallel arrays of Cy3-labeled oligonucleotide features generated from a 1D cantilever array. Reproduced with permission.[32] Copyright 2009, American Chemical Society. D) Patterning of Au NPs, Fe_2O_3 NPs and C_{60} by PEG-matrix-assisted DPN with varied dwell time. E) Fabrication of a C_{60} photoresponsive transistor by matrix-assisted DPN. F) Optical image of dot arrays made by matrix-assisted PPL over large areas, the insert showing an AFM image of a dot array written by a single pen. Reproduced with permission.[33] G) Direct writing of PEO- block -P2VP micelles loaded with $HAuCl_4$. H) SEM image of an array of sub-10-nm Au nanoparticles formed within the block-copolymer matrixes after plasma treatment; the insert shows a high-resolution TEM image of a single-crystalline Au nanoparticle. Reproduced with permission.[36] Copyright 2010, The National Academy of Sciences of the USA.

ferroelectric polymers, has played a core role in the fabrication of nanoelectronic devices, as well as in the study of electrical properties of polymers on the nanoscale. Both destructive and constructive SPL techniques have been used for integrating functional polymer nanostructures into devices, each focusing on specific materials.

Nanoscratching on polymer films by means of an AFM tip has been demonstrated as being an effective technique for patterning polymer electrodes (Figure 6A–B).[39] For instance, high density nanochannel arrays on poly(3,4-ethylenedioxythiophene):poly(4-styrenesulphonate) (PEDOT:PSS) thin films could be fabricated by nanoscratching to define polymer electrode pairs. After depositing a semiconducting layer on top of the electrodes, fabricated organic transistors, with varied channel lengths down to 100 nm, exhibited an excellent electronic performance. On the other hand, scratching the substrate surfaces with an AFM tip formed a trench with a high friction force, which permitted the confined synthesis of conducting polymer nanowires.[40] Chiang

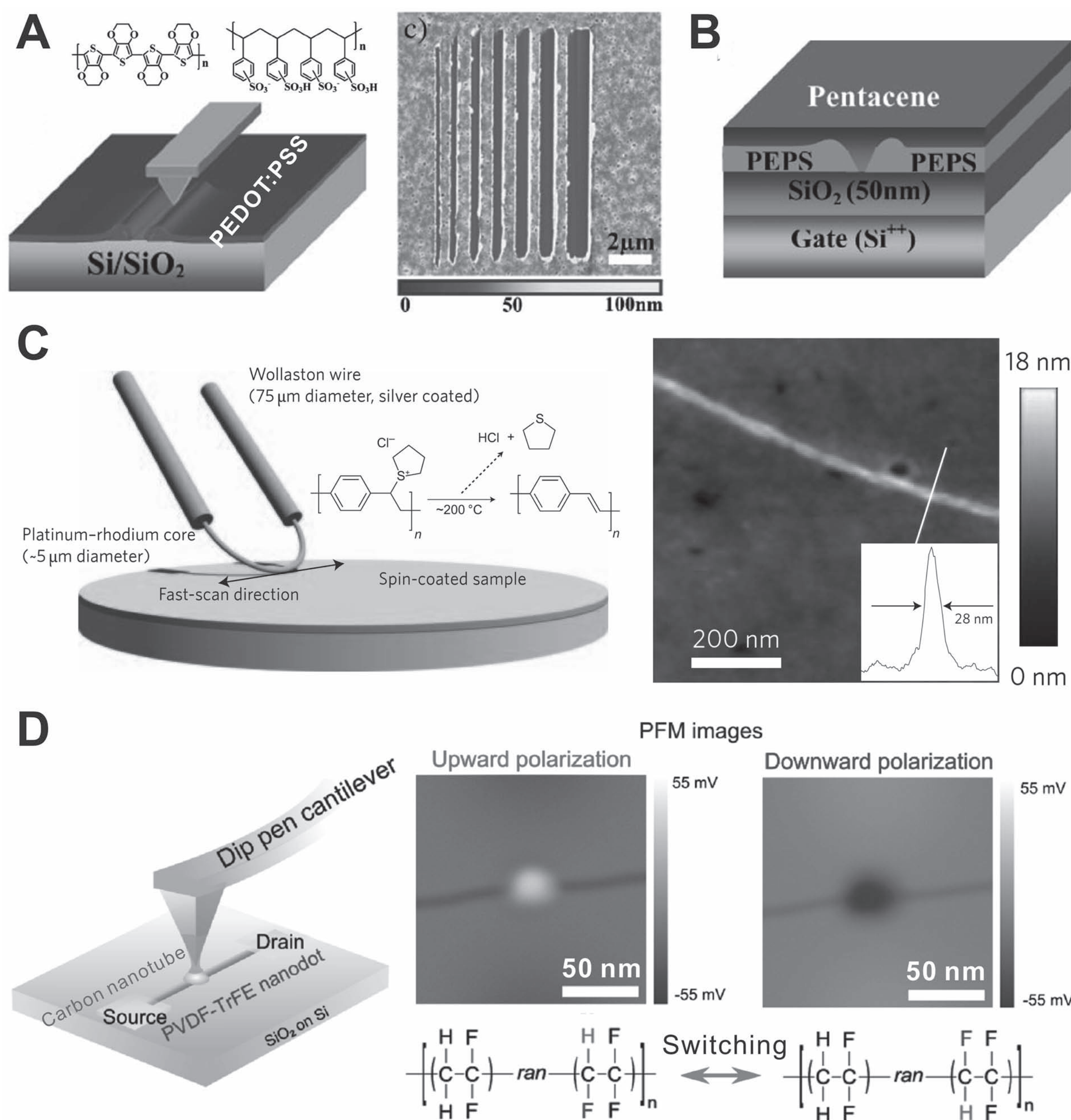

Figure 6. SPL-fabricated polymer electronic devices. A) Fabrication of polymer electrodes for organic transistors by nanoscratching, and an AFM image of scratched PEDOT:PSS channels with widths ranging from ≈100 nm to 900 nm. B) Schematic illustration of a pentacene thin-film transistor with PEDOT:PSS source/drain electrodes. Reproduced with permission.[39] C) Thermochemical writing of a 28 nm-wide PPV nanowire by a heated probe. Reproduced with permission.[41a] Copyright 2009, Nature Publishing Group. D) DPN of a ferroelectric PVDF-TrFE nanodot on a carbon nanotube for fabricating a non-volatile memory nanodevice. Piezoelectric force microscopy (PFM) was used to examine the piezoelectric characteristics of the nanodot. Reproduced with permission.[45] Copyright 2010 American Chemical Society.

© 2012 WILEY-VCH Verlag GmbH & Co. KGaA, Weinheim

and Wu demonstrated the fabrication of 15 nm-wide polyaniline nanowires on polymeric substrates.[40b] Such conjugated polymer chains confined in such narrow areas were found to have a high degree of alignment, which might lead to improved charge transport.[40a]

High-resolution SPL nanofabrication of polymer semiconductors has been recently demonstrated by introducing thermochemical or photochemical conversion. Nanopatterns of insoluble poly(p-phenylene vinylene) (PPV) were fabricated from its soluble salt precursor by fast scanning a heated probe on the surface of the precursor thin film, where the localized heat brought about thermochemical transformations in the PPV precursor (Figure 6C).[41] By rational control of the temperature and contact time, a record resolution below 28 nm was achieved.[41a] SNOL has also been demonstrated to spur the localized formation of PPV from its salt precursor, as well as the site-selective photo-crosslinking of a poly(9,9′-dioctylfluorene) (F8) derivative, producing patterns with resolution below 60 nm.[42]

DPN is also capable of patterning some conjugated polymers. However, only very thin nanostructures of conjugated polymers have been fabricated in previous reports[43] because of the inefficient transport of the polymers. Thermal DPN was used to pattern poly(3-dodecylthiophene) (PDDT) with an adequate thickness, where the monolayer-by-monolayer deposition of the PDDT was controlled by the writing speed and the tip temperature.[44] Utilizing heated probes, PDDT nanostructures thicker than 30 nm were fabricated between electrode pairs to study the conductance of the as-made nanostructures. More recently, DPN nanopatterning of a ferroelectric polymer, PVDF-TrFE, was demonstrated as a successful implementation of nanodevice fabrication. An individual nanodot of PVDF-TrFE was precisely placed at the center of a single-walled carbon nanotube channel, and it served as a gate dielectric in a nanoscale non-volatile memory device (Figure 6D).[45]

5. Polymer Brushes

Polymer brushes, polymers with one end tethered on a surface, are important functional materials for tailoring interfacial properties.[1b,46] They show remarkable environmental robustness and well-organized molecular configurations when compared with physisorbed bulk polymers. SPL is versatile for the control of the morphology and the functionalities of patterned polymer brushes across nanometer and micrometer length scales.[47] Functional polymer brush nanostructures fabricated by means of SPL have shown a wide range of applications. For example, responsive nanopatterned surfaces have been fabricated with either solvent-sensitive[48] or pH-sensitive[49] brushes. Not only can the reversible switching of the chain conformation be studied at the nanometer level, but also surface actuation can be triggered to hide/unveil functional surfaces.[48b] Polymer brushes serve as functional interfaces for biological applications such as cell adhesion and protein immobilization;[50] for instance, PEG and poly(oligo(ethylene glycol) methacrylate) (POEGMA) brushes are commonly used as protein-resistant surfaces. Nanopatterning of brushes using SPL, especially with the use of cantilever arrays, has provided a low-cost, bench-top preparation method for fabricating biochips composed of protein nanoarrays.[51] Since polymer brushes are also suitable for loading nanomaterials, the nanostructures of polymer brushes have been applied in nanosensors[52] and electronic devices.[53]

The mainstream of research in the fabrication of nanostructures of polymer brushes is the site-selective immobilization of molecular initiators on a substrate by SPL, combined with subsequent surface-initiated polymerization (SIP) from the initiators.[50,54] This method, also called "*grafting from*", is seen to be effective with the capability of controlling the molecular weight, dimensions, chain configuration and composition of brushes. Previous examples include nanoshaving with atom-transfer radical polymerization (ATRP),[48a] AFM electro-oxidation with ring-opening metathesis polymerization (ROMP),[55] nanografting with photopolymerization,[56] and DPN with various SIPs.[57]

Very recently, we developed a new SPL technique, namely dip-pen nanodisplacement lithography (DNL), for programming patterned nanostructures of polymer brushes (Figure 7).[58] In DNL, an AFM tip inked with ω-mercaptoundecyl bromoisobutyrate (MUDBr) initiator molecules was used to indent or shave a Au surface precoated with an inert self-assembled monolayer (SAM) of 16-mercaptohexadecanoic acid (MHA), during which the MHA molecules were eliminated at a higher load, along with displacement by the MUDBr. As a variant of DPN, DNL has several distinct features. Firstly, since the volatile MUDBr molecules quickly assemble on the exposed areas without the need of a water meniscus, high-speed writing is possible, free from the humidity-controlled ink transport in DPN. Secondly, ink diffusion is prohibited by the surrounding dense SAMs, leading to nanofeatures as small as 25 nm. The size is restricted only by the curvature of the tip and the crystallization quality of the Au substrate. In principle, sharper tips and a single-crystalline Au substrates can yield smaller features. After DNL, poly[2-(methacryloyloxy)-ethyltrimethylammonium chloride] (PMETAC) brushes were grown from initiator templates using surface-initiated ATRP (SI-ATRP). We found that the shape of the nanobrushes was droplet-like and the lateral size and height were determined by the initiator footprints. Smaller initiator patterns afford plenty

© 2012 WILEY-VCH Verlag GmbH & Co. KGaA, Weinheim

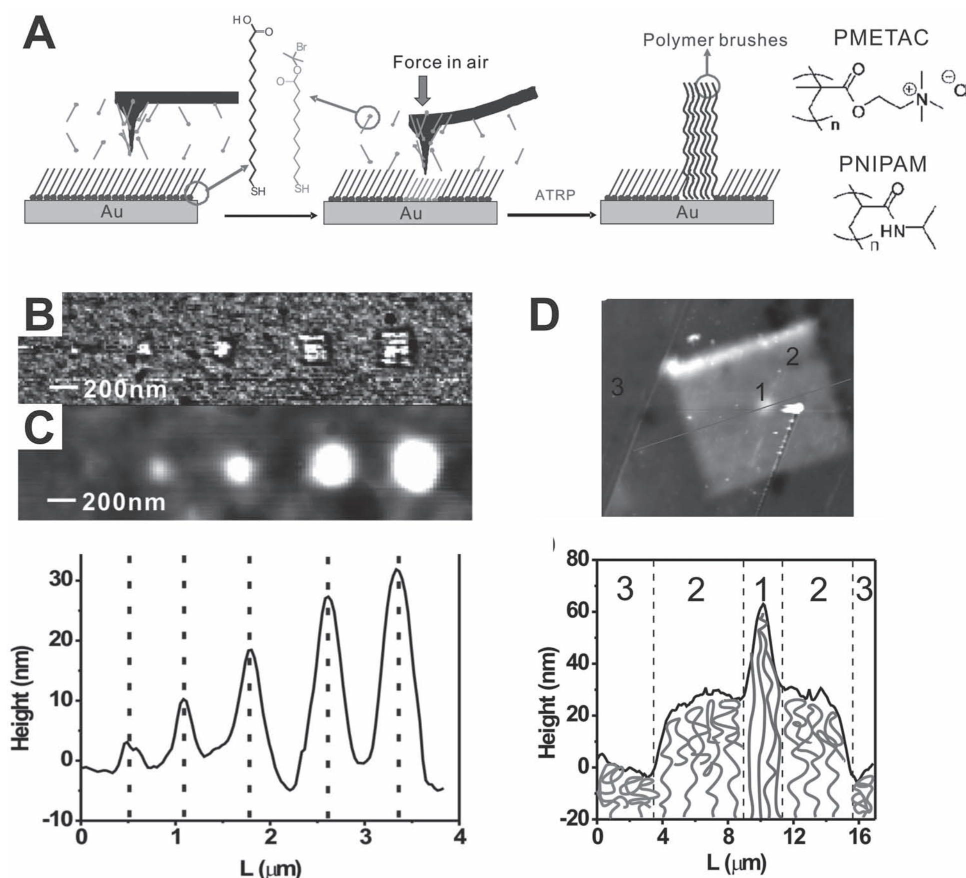

Figure 7. Programmable nanostructures of polymer brushes fabricated by DNL. A) Schematic illustration of the DNL patterning and site-selective growth of polymer brushes. B) AFM lateral force image of MUDBr with different feature sizes made by DNL. C) AFM topographic image of PMETAC brushes grown from the MUDBr initiator features in Figure 7B and the corresponding cross-sectional profiles. D) Control of the thickness and the chain configuration of PMETAC brushes by varying the grafting density. Reproduced with permission.[58] Copyright 2010, The Royal Society of Chemistry.

of room for the relaxing and spreading of brush chains on the substrate, leading to a decrease in brush height. The brush height also depends on the force applied during DNL. This is because more MHA molecules are displaced by MUDBr at higher applied forces, leading to a higher chain-grafting density. Notably, the surface Br-initiator can be terminated and a second displacement is allowed for multiplexed polymer brushes.

More importantly, we discovered that the height and shape of the nanobrushes is a function of the lateral distance between neighboring features. We utilized DNL to precisely control the distance between the initiator features from 1000 nm to 25 nm, and found a morphological transition from isolated to bridged to planar structures with decreasing lateral space (Figure 8A).[59] This discovery led to the invention of a " feature-density" method for the fabrication of 3D patterned polymer brushes. In this method, the key step is to fabricate arrays of nanodots of polymer brushes with controlled dot-to-dot spacing. This is realized by the DNL-writing of an "initiator bitmap" with a defined pixel number and pixel distance, on the basis of a white/black bitmap that is converted from a gray-scale image, and by the subsequent growth of PMETAC brushes via SI-ATRP from the "initiator bitmap". As a result, the density and positioning information of the bitmap can be transferred into 3D structures (Figure 8B). Compared with the use of a single chain as the building block in traditional polymerization-time and grafting-density methods, the feature-density method uses nanofeatures as building blocks, and therefore it can effectively simplify the fabrication process (i.e., shorter time and fewer lithographic steps).[60] Furthermore, we have developed the feature-density approach into a parallel writing fashion. Figure 8C shows an array of PMETAC brushes patterns that were fabricated in parallel using an 18-tip cantilever array (unpublished result).

Apart from "*grafting from*" strategies, some alternative routes for SPL-based fabrication of brush nanostructures have also been reported recently. For instance, destructive SPL is feasible for directly structuring pregrown brush

© 2012 WILEY-VCH Verlag GmbH & Co. KGaA, Weinheim

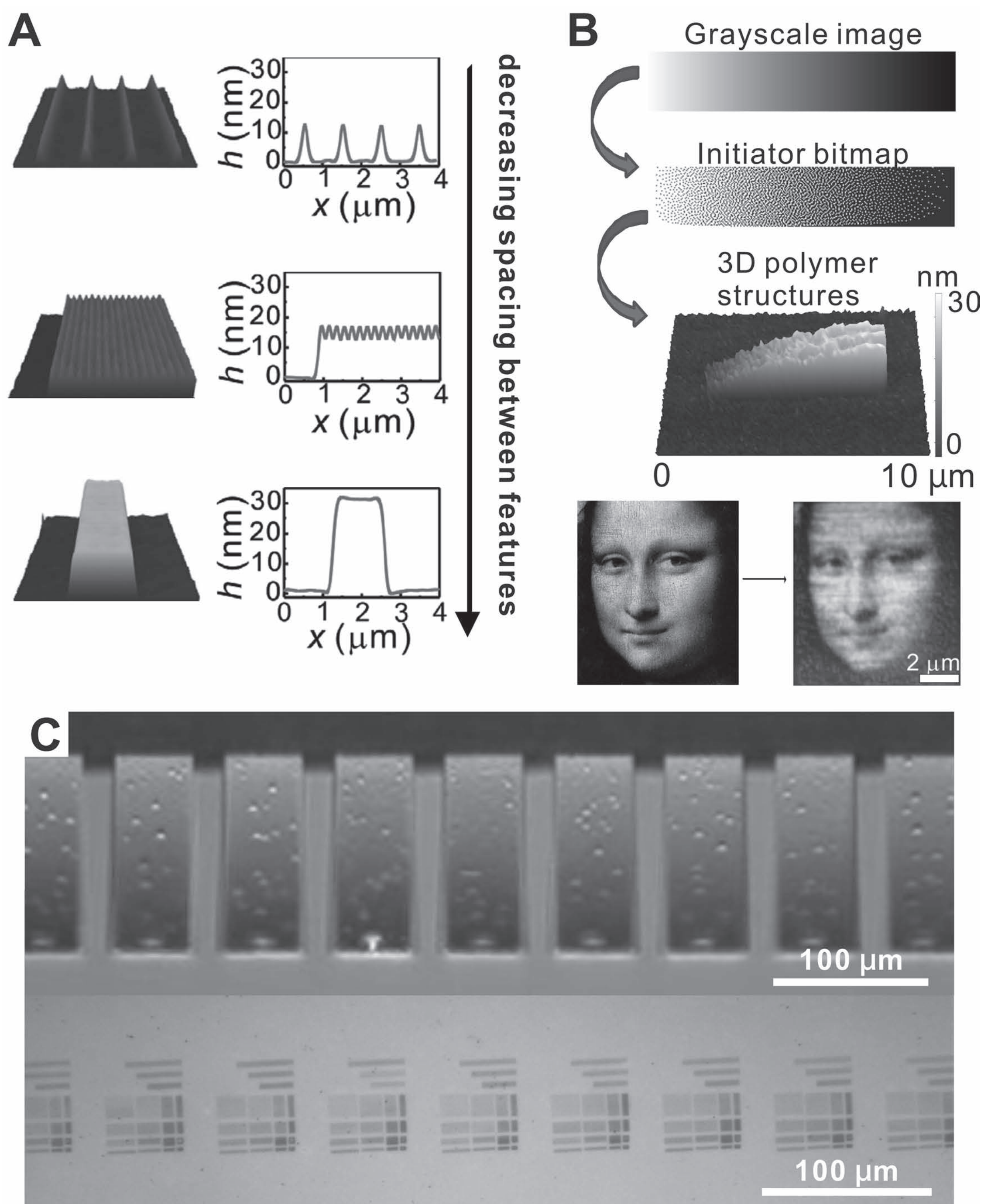

Figure 8. 3D polymer-brush nanostructures made by DNL. A) The evolution of brush height at different distance between nanobrushes. B) The feature-density method for fabricating arbitrary 3D patterned polymer brushes from DNL and SI-ATRP. Reproduced with permission.[59] C) Parallelly fabricated 3D patterned polymer brush nanostructures by using an 18-tip 1D cantilever array.

films via scratching,[61] photodegradation[51a] or electrochemical oxidation.[62] For example, high-load-force AFM lithography was found to be a simple means of fabricating polymer brush nanotemplates by scratching a layer of pregrafted brushes prepared by means of SIP.[61] Nanostructured polystyrene (PS) and poly(n-butyl acrylate) (PNBA) brushes prepared using this method were further exploited for site specific immobilization of proteins over large areas by utilizing a cantilever array.[51c] An electrochemical AFM tip was also applied for local electrografting of vinylic monomers on conducting substrates with *the initiators generated* in situ.[63]

© 2012 WILEY-VCH Verlag GmbH & Co. KGaA, Weinheim

6. Summary of the Attributes of SPL Techniques

SPL-based fabrication of polymer nanostructures for different applications is summarized in Table 1. All of the SPL examples show the capability of fabricating polymer nanostructures with sizes spanning from tens of nanometers to many micrometers in a serial patterning fashion. Generally, the minimal feature sizes made by destructive SPL methods are smaller than those by constructive ones. The smallest feature size reported to date is ≈10 nm, achieved using thermomechanical nanolithography.[23] This performance has exceeded the capability of conventional photolithography and is close to that of e-beam lithography (EBL), nanoimprint lithography (NIL) and block copolymer (BCP) nanolithography.

Since all SPL techniques are serial patterning process, they are very powerful tools for creating complex polymer nanostructures with well-controlled position, shape and size, making them preferable to nanolithographic tools such as photolithography, NIL and BCP nanolithography. Of the many SPL techniques, thermochemical nanolithography and DNL have demonstrated the power of creating arbitrary 3D polymer structures with nanometer resolution in all dimensions, in addition to having the capability of generating 2D polymer nanoarrays. Also, the same SPL tool can be used for scanning probe microscopy imaging purposes. This attribute is essentially important for patterning multiplexed nanostructures, because one can readily align the second pattern to the previous one. By way of comparison, other nanolithographic techniques typically require markers for realignment, which dramatically increases the complication, as well as decreasing the registration, of the multiplexed patterning.

From a material-compatibility perspective, SPL shows a high level of flexibility (chemical or physical, constructive or destructive, ambient or environmental-controlled) in nanopatterning different polymeric materials and even inorganic materials using a polymer-matrix system, which is a unique advantage over other nanopatterning methods, such as photolithography, EBL, NIL and BCP nanolithography. More importantly, the direct writing of polymer nanostructures at ambient conditions by SPL techniques such as DPN avoids the use of toxic solvents, high-energy exposure and etching steps that are typically found in conventional nanolithography techniques. Therefore, SPL is more suitable for patterning bio-macromolecules and conjugated polymers.

Most SPL techniques have been demonstrated using a single tip, and therefore the throughput is relatively low (<10^{-10} m^2 s^{-1} as patterned by a single tip). The throughput can be dramatically increased by using 1D cantilever arrays (thermomechanical indentation, nanoscratching of polymer brushes, Snomipede, DPN and DNL), 2D cantilever arrays (thermomechanical indentation and DPN), or 2D cantilever-free polymer-pen arrays (PPL and BPL). Of

Table 1. Summary of polymer materials made by SPL.

Material Applications	Materials	SPL Methods	Chemical/Physical SPL	Resolution	Parallelization
Polymer resists	positive photoresist[20–22]	SNOL, Snomipede, BPL	chemical: photochemical degradation	35nm,[20] 100 nm[22]	1D cantilever array, 2D polymer - pen array
	PMMA,[18a] cross-linked polyaryletherketone[23]	thermomechanical indentation	physical: heat-assisted elastic deformation	≈10 nm	2D cantilever array
	phthalaldehyde SAD polymers[24,25]	thermochemical nanolithography	chemical: thermal decomposition	≈40 nm lateral and 1 nm vertical	single tip
	PEG,[27–30] PDMS[31]	DPN, PPL	physical: physisorption of liquid polymer inks	hundreds of nanometers to micrometer	1D cantilever array, 2D polymer - pen array
Polymeric carriers for functional materials	agarose,[32] PEG,[33,34] PEO-block -P2VP,[36] photocurable photoresist[38]	DPN, PPL	physical or chemical: physisorption of polymer matrix, chemical binding of biomolecules	hundreds of nanometers to micrometer	1D cantilever array, 2D polymer - pen array
	water-insoluble polymers[37]	thermal DPN	physical: melt of polymer nanocomposites and physisorption	hundreds of nanometers	single tip

© 2012 WILEY-VCH Verlag GmbH & Co. KGaA, Weinheim

Table 1. Continued.

Material Applications	Materials	SPL Methods	Chemical/Physical SPL	Resolution	Parallelization
Electronically active polymers	PEDOT:PSS,[39] polypyrrole,[40a] polyaniline,[40b]	nanoscratching	physical: mechanical scratching of the surface	100 nm,[39] 15 nm[40b]	single tip
	PPV[41,42]	thermochemical nanolithography, SNOL	chemical: thermo-/photochemical conversion from the soluble salt precursor	28 nm,[41a] ≈50 nm[42]	single tip
	crosslinkable F8 derivatives[42]	SNOL	chemical: photo-crosslinking	60 nm	single tip
	water-soluble conjugated polymers,[43] PVDF-TrFE[45]	DPN,	physical: physisorption	130 nm for conjugated polymers,[43a] 19 nm for PVDF-TrFE[45]	single tip
	PDDT[44]	thermal DPN	physical: melting of polymers and physisorption	<80 nm	single tip
Polymer brushes	Poly(***N*** - isopropylacrylamide) (PNIPAM), PMMA, etc.,[48] PS, PNIPAM and PNBA[51c,61]	nanoshaving, nanoscratching	physical: mechanical scratching of the surface layer[48] or brush film[51c,61]	100 nm	1D cantilever array
	photopolymerization of coumarin-derivative thiols[56]	nanografting	chemical: nanografting of the thiol monomers	40 nm	single tip
	PEG,[51b] PMAA, polypeptide, etc.[57]	DPN	chemical: transport and chemical immobilization of initiators	hundreds of nanometers	single tip
	PMETAC, PNIPAM[58]	DNL	chemical: nanoscale displacement of the thiol SAM molecules	initiator: 25 nm brushes: ≈100 nm	1D cantilever array
	PMPC[21] POEGMA[51a]	SNOL	chemical: photodegradation of SAMs or brushes	≈200 nm	1D cantilever array
	PHEMA,[49] polymer brushes by ROMP,[55] PAA, PNIPAM, POEGMA etc.,[62] PAA[63]	AFM electrochemical oxidation	chemical: electrochemical oxidation of the substrate,[49,55] brush film[62] or initiators[63]	40 nm,[49,62] ≈200 nm[63]	single tip

the many examples, DPN and its derivatives are the most frequently reported tools for parallel patterning. The parallelization route has rendered SPL as potentially competitive with other serial nanolithographic tools, such as industrial EBL. Compared with parallel nanolithographic tools, such as photolithography and NIL, however, the throughput of parallel SPLs at the current stage is still relatively low.

In terms of the cost of the equipment, SPL is more cost effective than photolithography and EBL, which require expensive apparatus and are operated in cleanrooms. The equipment for SPL, however, is commonly used in materials characterization and the operation conditions are typically ambient except for some specific cases. With the application of cantilever and polymer pen arrays, the unit cost of making polymer nanostructures using SPL can be

© 2012 WILEY-VCH Verlag GmbH & Co. KGaA, Weinheim

substantially lower than that for EBL. This is particularly true in the case of constructive SPL techniques, in which the “inks” can be ≈100% delivered as the final functional nanostructures.

7. Conclusion and Outlook

In recent developments, polymer materials patterned by SPL not only passively serve as fabrication resists and carrier matrices for embedded functional materials, they also act as active components for surface engineering and electronic devices. We believe that these demonstrations show the future potential of SPL as a low-cost, bench-top, and flexible tool for making polymer nanostructures for a wide variety of purposes. For polymer-based nanofabrication, SPL can become a powerful, low-cost technique for making patterned resists for many functional materials. It can also be used to fabricate photomasks for photolithography and phase-shift lithography. This may be particularly interesting to academic researchers because of the economic and flexible advantages. Because SPL typically does not involve complicated fabrication steps, toxic solvents or strong energy, it is especially suitable for patterning biological materials and some functional polymers for device applications. In particular, the development of carrier matrices and brush templates may provide solutions to apply the technique to materials that are not traditionally processed using SPL. SPL offers unique opportunities for studying and controlling the structures and properties of polymers at the nanometer and even molecular levels. Nanodevices and responsive interfaces with polymer brushes can be constructed by means of SPL with precise control of the dimensions, molecular organization and functions. All of the applications require a reproducible and high-throughput SPL tool. The development of parallel SPL techniques using cantilever arrays and cantilever-free tip arrays is a critical issue in the future. Although improvements are still required in areas such as patterning efficiency, uniformity and applicability to more systems,[64] we are confident that SPL will spur more advances in fundamental research and technological development for practical applications of polymer nanostructures in the future.

Acknowledgements: Z. J. Z. acknowledges The Hong Kong Polytechnic University (Projects 1-ZV5Z, A-PK09, A-PK21) and the Research Grant Council of Hong Kong (Project PolyU 5041/11P) for financial support of this work. We acknowledge Prof. Gail Taylor for her generous help in proof-reading and correcting the language of this article.

Received: November 12, 2011; Revised: December 9, 2011; Published online: February 8, 2012; DOI: 10.1002/marc.201100761

Keywords: nanotechnology; parallelization; polymer nanostructures; scanning probe lithography; surface patterning

[1] a) Z. H. Nie, E. Kumacheva, *Nat. Mater.* **2008**, *7*, 277; b) M. A. C. Stuart, W. T. S. Huck, J. Genzer, M. Muller, C. Ober, M. Stamm, G. B. Sukhorukov, I. Szleifer, V. V. Tsukruk, M. Urban, F. Winnik, S. Zauscher, I. Luzinov, S. Minko, *Nat. Mater.* **2010**, *9*, 101.
[2] a) D. Wouters, U. S. Schubert, *Angew. Chem. Int. Ed.* **2004**, *43*, 2480; b) A. A. Tseng, A. Notargiacomo, T. P. Chen, *J. Vac. Sci. Technol. B* **2005**, *23*, 877; c) R. Garcia, R. V. Martinez, J. Martinez, *Chem. Soc. Rev.* **2006**, *35*, 29; d) A. A. Tseng, S. Jou, A. Notargiacomo, T. P. Chen, *J. Nanosci. Nanotechnol.* **2008**, *8*, 2167.
[3] a) K. Salaita, Y. H. Wang, C. A. Mirkin, *Nature Nanotechnol.* **2007**, *2*, 145; b) X. Z. Zhou, F. Boey, F. W. Huo, L. Huang, H. Zhang, *Small* **2011**, *7*, 2273.
[4] a) L. Sohn, R. Willett, *Appl. Phys. Lett.* **1995**, *67*, 1552; b) U. Kunze, B. Klehn, *Adv. Mater.* **1999**, *11*, 1473; c) M. Heyde, K. Rademann, B. Cappella, M. Geuss, H. Sturm, T. Spangenberg, H. Niehus, *Rev. Sci. Instrum.* **2001**, *72*, 136.
[5] S. Xu, G. Liu, *Langmuir* **1997**, *13*, 127.
[6] H. Mamin, D. Rugar, *Appl. Phys. Lett.* **1992**, *61*, 1003.
[7] a) S. Bakbak, P. J. Leech, B. E. Carson, S. Saxena, W. P. King, U. H. F. Bunz, *Macromolecules* **2006**, *39*, 6793; b) B. Gotsmann, U. Duerig, J. Frommer, C. J. Hawker, *Adv. Funct. Mater.* **2006**, *16*, 1499; c) R. Szoszkiewicz, T. Okada, S. C. Jones, T. D. Li, W. P. King, S. R. Marder, E. Riedo, *Nano Lett.* **2007**, *7*, 1064.
[8] a) S. F. Lyuksyutov, R. A. Vaia, P. B. Paramonov, S. Juhl, L. Waterhouse, R. M. Ralich, G. Sigalov, E. Sancaktar, *Nat. Mater.* **2003**, *2*, 468; b) S. Jegadesan, S. Sindhu, S. Valiyaveettil, *Small* **2006**, *2*, 481.
[9] a) D. Wouters, S. Hoeppener, U. S. Schubert, *Angew. Chem. Int. Ed.* **2009**, *48*, 1732; b) S. Y. Jang, M. Marquez, G. A. Sotzing, *J. Am. Chem. Soc.* **2004**, *126*, 9476; c) S. Jagadesan, R. C. Advincula, S. Valiyaveettil, *Adv. Mater.* **2005**, *17*, 1282.
[10] a) S. Wegscheider, A. Kirsch, J. Mlynek, G. Krausch, *Thin Solid Films* **1995**, *264*, 264; b) A. Naber, H. Kock, H. Fuchs, *Scanning* **1996**, *18*, 567; c) G. J. Leggett, S. Q. Sun, K. S. L. Chong, *J. Am. Chem. Soc.* **2002**, *124*, 2414.
[11] R. D. Piner, J. Zhu, F. Xu, S. H. Hong, C. A. Mirkin, *Science* **1999**, *283*, 661.
[12] D. S. Ginger, H. Zhang, C. A. Mirkin, *Angew. Chem. Int. Ed.* **2004**, *43*, 30.
[13] N. A. Amro, S. Xu, G. Y. Liu, *Langmuir* **2000**, *16*, 3006.
[14] P. Sheehan, L. Whitman, W. P. King, B. A. Nelson, *Appl. Phys. Lett.* **2004**, *85*, 1589.
[15] B. W. Maynor, S. F. Filocamo, M. W. Grinstaff, J. Liu, *J. Am. Chem. Soc.* **2002**, *124*, 522.
[16] K. H. Kim, N. Moldovan, H. D. Espinosa, *Small* **2005**, *1*, 632.
[17] W. K. Lee, P. E. Sheehan, *Scanning* **2008**, *30*, 172.
[18] a) P. Vettiger, M. Despont, U. Drechsler, U. Durig, W. Haberle, M. I. Lutwyche, H. E. Rothuizen, R. Stutz, R. Widmer, G. K. Binnig, *IBM J. Res. Dev.* **2000**, *44*, 323; b) S. Hong, C. A. Mirkin, *Science* **2000**, *288*, 1808; c) K. Salaita, S. W. Lee, X. F. Wang, L. Huang, T. M. Dellinger, C. Liu, C. A. Mirkin, *Small* **2005**, *1*, 940; d) K. Salaita, Y. H. Wang, J. Fragala, R. A. Vega, C. Liu, C. A. Mirkin, *Angew. Chem. Int. Ed.* **2006**, *45*, 7220; e) C. A. Mirkin, *ACS Nano* **2007**, *1*, 79; f) C. Liu, *Mater. Today* **2008**, *11*, 22.
[19] a) F. W. Huo, Z. J. Zheng, G. F. Zheng, L. R. Giam, H. Zhang, C. A. Mirkin, *Science* **2008**, *321*, 1658; b) X. Liao, A. B. Braunschweig, Z. J. Zheng, C. A. Mirkin, *Small* **2010**, *6*, 1082; c) X. Liao, A. B. Braunschweig, C. A. Mirkin, *Nano Lett.* **2010**, *10*, 1335; d) W. Shim, A. B. Braunschweig, X. Liao, J. Chai, J. K. Lim, G. Zheng, C. A. Mirkin, *Nature* **2011**, *469*,

© 2012 WILEY-VCH Verlag GmbH & Co. KGaA, Weinheim

516; e) L. R. Giam, C. A. Mirkin, *Angew. Chem. Int. Ed.* **2011**, *50*, 7482.
[20] J. W. Kingsley, S. K. Ray, A. M. Adawi, G. J. Leggett, D. G. Lidzey, *Appl. Phys. Lett.* **2008**, *93*, 213103.
[21] E. u. Haq, Z. Liu, Y. Zhang, S. A. A. Ahmad, L.-S. Wong, S. P. Armes, J. K. Hobbs, G. J. Leggett, J. Micklefield, C. J. Roberts, J. M. R. Weaver, *Nano Lett.* **2010**, *10*, 4375.
[22] F. W. Huo, G. F. Zheng, X. Liao, L. R. Giam, J. A. Chai, X. D. Chen, W. Y. Shim, C. A. Mirkin, *Nature Nanotechnol.* **2010**, *5*, 637.
[23] a) T. Altebaeumer, B. Gotsmann, H. Pozidis, A. Knoll, U. Duerig, *Nano Lett.* **2008**, *8*, 4398; b) D. Wiesmann, C. Rawlings, R. Vecchione, F. Porro, B. Gotsmann, A. Knoll, D. Pires, U. Duerig, *Nano Lett.* **2009**, *9*, 3171; c) B. Gotsmann, A. W. Knoll, R. Pratt, J. Frommer, J. L. Hedrick, U. Duerig, *Adv. Funct. Mater.* **2010**, *20*, 1276.
[24] a) O. Coulembier, A. Knoll, D. Pires, B. Gotsmann, U. Duerig, J. Frommer, R. D. Miller, P. Dubois, J. L. Hedrick, *Macromolecules* **2010**, *43*, 572; b) F. Holzner, C. Kuemin, P. Paul, J. L. Hedrick, H. Wolf, N. D. Spencer, U. Duerig, A. W. Knoll, *Nano Lett.* **2011**, *11*, 3957.
[25] A. W. Knoll, D. Pires, O. Coulembier, P. Dubois, J. L. Hedrick, J. Frommer, U. Duerig, *Adv. Mater.* **2010**, *22*, 3361.
[26] a) D. Pires, J. L. Hedrick, A. De Silva, J. Frommer, B. Gotsmann, H. Wolf, M. Despont, U. Duerig, A. W. Knoll, *Science* **2010**, *328*, 732; b) Y. D. Yan, Z. J. Hu, X. S. Zhao, T. Sun, S. Dong, X. D. Li, *Small* **2010**, *6*, 724.
[27] R. G. Sanedrin, L. Huang, J. W. Jang, J. Kakkassety, C. A. Mirkin, *Small* **2008**, *4*, 920.
[28] J. W. Jang, R. G. Sanedrin, A. J. Senesi, Z. J. Zheng, X. D. Chen, S. Hwang, L. Huang, C. A. Mirkin, *Small* **2009**, *5*, 1850.
[29] Z. J. Zheng, J. W. Jang, G. Zheng, C. A. Mirkin, *Angew. Chem. Int. Ed.* **2008**, *47*, 9951.
[30] J. W. Jang, Z. J. Zheng, O. S. Lee, W. Shim, G. F. Zheng, G. C. Schatz, C. A. Mirkin, *Nano Lett.* **2010**, *10*, 4399.
[31] A. Hernandez-Santana, E. Irvine, K. Faulds, D. Graham, *Chem. Sci.* **2011**, *2*, 211.
[32] A. J. Senesi, D. I. Rozkiewicz, D. N. Reinhoudt, C. A. Mirkin, *ACS Nano* **2009**, *3*, 2394.
[33] L. Huang, A. B. Braunschweig, W. Shim, L. D. Qin, J. K. Lim, S. J. Hurst, F. W. Huo, C. Xue, J. W. Jong, C. A. Mirkin, *Small* **2010**, *6*, 1077.
[34] H. Li, Q. Y. He, X. H. Wang, G. Lu, C. Liusman, B. Li, F. Boey, S. S. Venkatraman, H. Zhang, *Small* **2011**, *7*, 226.
[35] a) S. Lenhert, P. Sun, Y. Wang, H. Fuchs, C. A. Mirkin, *Small* **2007**, *3*, 71; b) S. Sekula, J. Fuchs, S. Weg-Remers, P. Nagel, S. Schuppler, J. Fragala, N. Theilacker, M. Franueb, C. Wingren, P. Ellmark, C. A. K. Borrebaeck, C. A. Mirkin, H. Fuchs, S. Lenhert, *Small* **2008**, *4*, 1785; c) S. Lenhert, F. Brinkmann, T. Laue, S. Walheim, C. Vannahme, S. Klinkhammer, M. Xu, S. Sekula, T. Mappes, T. Schimmel, H. Fuchs, *Nature Nanotechnol.* **2010**, *5*, 275; d) Z. J. Zheng, W. L. Daniel, L. R. Giam, F. W. Huo, A. J. Senesi, G. F. Zheng, C. A. Mirkin, *Angew. Chem. Int. Ed.* **2009**, *48*, 7626.
[36] J. A. Chai, F. W. Huo, Z. J. Zheng, L. R. Giam, W. Shim, C. A. Mirkin, *Proc. Natl. Acad. Sci. USA* **2010**, *107*, 20202.
[37] W. K. Lee, Z. T. Dai, W. P. King, P. E. Sheehan, *Nano Lett.* **2010**, *10*, 129.
[38] A. Hernandez-Santana, A. R. Mackintosh, B. Guilhabert, A. L. Kanibolotsky, M. D. Dawson, P. J. Skabara, D. Graham, *J. Mater. Chem.* **2011**, *21*, 14209.
[39] L. Li, M. Hirtz, W. Wang, C. Du, H. Fuchs, L. Chi, *Adv. Mater.* **2010**, *22*, 1374.
[40] a) M. Woodson, J. Liu, *J. Am. Chem. Soc.* **2006**, *128*, 3760; b) C.-H. Chiang, C.-G. Wu, *Chem. Commun.* **2010**, *46*, 2763.
[41] a) O. Fenwick, L. Bozec, D. Credgington, A. Hammiche, G. M. Lazzerini, Y. R. Silberberg, F. Cacialli, *Nature Nanotechnol.* **2009**, *4*, 664; b) D. B. Wang, S. Kim, W. D. Underwood, A. J. Giordano, C. L. Henderson, Z. T. Dai, W. P. King, S. R. Marder, E. Riedo, *Appl. Phys. Lett.* **2009**, *95*, 233108.
[42] D. Credgington, O. Fenwick, A. Charas, J. Morgado, K. Suhling, F. Cacialli, *Adv. Funct. Mater.* **2010**, *20*, 2842.
[43] a) J. H. Lim, C. A. Mirkin, *Adv. Mater.* **2002**, *14*, 1474; b) A. Noy, A. E. Miller, J. E. Klare, B. L. Weeks, B. W. Woods, J. J. DeYoreo, *Nano Lett.* **2002**, *2*, 109; c) Q. Tang, S. Q. Shi, *Sens. Actuators B* **2008**, *131*, 379.
[44] a) M. Yang, P. E. Sheehan, W. P. King, L. J. Whitman, *J. Am. Chem. Soc.* **2006**, *128*, 6774; b) A. R. Laracuente, M. Yang, W. K. Lee, L. Senapati, J. W. Baldwin, P. E. Sheehan, W. P. King, S. C. Erwin, L. J. Whitman, *J. Appl. Phys.* **2010**, *107*, 103723.
[45] J. Y. Son, S. Ryu, Y. C. Park, Y. T. Lim, Y. S. Shin, Y. H. Shin, H. M. Jang, *ACS Nano* **2010**, *4*, 7315.
[46] P. Uhlmann, H. Merlitz, J. U. Sommer, M. Stamm, *Macromol. Rapid Commun.* **2009**, *30*, 732.
[47] X. Sui, S. Zapotoczny, E. M. Benetti, P. Schon, G. J. Vancso, *J. Mater. Chem.* **2010**, *20*, 4981.
[48] a) M. Kaholek, W. K. Lee, B. LaMattina, K. C. Caster, S. Zauscher, *Nano Lett.* **2004**, *4*, 373; b) J. P. S. Badyal, S. Morsch, W. C. E. Schofield, *Langmuir* **2010**, *26*, 12342.
[49] E. M. Benetti, H. J. Chung, G. J. Vancso, *Macromol. Rapid Commun.* **2009**, *30*, 411.
[50] R. Barbey, L. Lavanant, D. Paripovic, N. Schuwer, C. Sugnaux, S. Tugulu, H. A. Klok, *Chem. Rev.* **2009**, *109*, 5437.
[51] a) S. A. A. Ahmad, A. Hucknall, A. Chilkoti, G. J. Leggett, *Langmuir* **2010**, *26*, 9937; b) T. Rakickas, E. M. Ericsson, Ž. Ružele˙, B. Liedberg, R. Valiokas, *Small* **2011**, *7*, 2153; c) H. Wagner, Y. Li, M. Hirtz, L. Chi, H. Fuchs, A. Studer, *Soft Matter* **2011**, *7*, 9854.
[52] S. Gupta, M. Agrawal, P. Uhlmann, F. Simon, U. Oertel, M. Stamm, *Macromolecules* **2008**, *41*, 8152.
[53] a) O. Azzaroni, Z. J. Zheng, Z. Q. Yang, W. T. S. Huck, *Langmuir* **2006**, *22*, 6730; b) Z. L. Liu, H. Y. Hu, B. Yu, M. A. Chen, Z. J. Zheng, F. Zhou, *Electrochem. Commun.* **2009**, *11*, 492; c) X. Wang, H. Hu, Y. Shen, X. Zhou, Z. J. Zheng, *Adv. Mater.* **2011**, *23*, 3090.
[54] A. Olivier, F. Meyer, J.-M. Raquez, P. Damman, P. Dubois, *Prog. Polym. Sci.*2012, *37*, 157.
[55] W. K. Lee, K. C. Caster, J. Kim, S. Zauscher, *Small* **2006**, *2*, 848.
[56] M. Barczewski, S. Walheim, T. Heiler, A. Blaszczyk, M. Mayor, T. Schimmel, *Langmuir* **2010**, *26*, 3623.
[57] a) X. G. Liu, S. W. Guo, C. A. Mirkin, *Angew. Chem. Int. Ed.* **2003**, *42*, 4785; b) S. Zapotoczny, E. M. Benetti, G. J. Vancso, *J. Mater. Chem.* **2007**, *17*, 3293; c) X. Z. Zhou, Y. H. Chen, B. Li, G. Lu, F. Y. C. Boey, J. Ma, H. Zhang, *Small* **2008**, *4*, 1324.
[58] X. Liu, Y. Li, Z. J. Zheng, *Nanoscale* **2010**, *2*, 2614.
[59] X. C. Zhou, X. L. Wang, Y. D. Shen, Z. Xie, Z. J. Zheng, *Angew. Chem. Int. Ed.* **2011**, *50*, 6506.
[60] X. Zhou, X. Liu, Z. Xie, Z. J. Zheng, *Nanoscale* **2011**, *3*, 4929.
[61] M. Hirtz, M. K. Brinks, S. Miele, A. Studer, H. Fuchs, L. Chi, *Small* **2009**, *5*, 919.
[62] R. Ferris, A. Hucknall, B. S. Kwon, T. Chen, A. Chilkoti, S. Zauscher, *Small* **2011**, *7*, 3032.
[63] J. Charlier, A. Ghorbal, F. Grisotto, S. Palacin, C. Goyer, C. Demaille, *ChemPhysChem* **2009**, *10*, 1053.
[64] A. A. Tseng, *Nano Today* **2011**, *6*, 493.

© 2012 WILEY-VCH Verlag GmbH & Co. KGaA, Weinheim